Meteoritics 29, 349–361 (1994

Basalt generation at the Apollo 12 site, Part 2: Source heterogeneity, multiple melts, and crustal contamination

CLIVE R. NEAL[1], MATTHEW D. HACKER[1,2], GREGORY A. SNYDER[3], LAWRENCE A. TAYLOR[3], YUN-GANG LIU[4], AND ROMAN A. SCHMITT[4]

[1]Department of Civil Engineering and Geological Sciences, University of Notre Dame, Notre Dame, Indiana 46556, USA
[2]Department of Earth and Space Sciences, University of California, Los Angeles, California 90024, USA
[3]Department of Geological Sciences, University of Tennessee, Knoxville, Tennessee 37996, USA
[4]Department of Chemistry and The Radiation Center, Oregon State University, Corvallis, Oregon 97331, USA

(Received 1993 July 29; accepted in revised form 1994 February 17)

Abstract–The petrogenesis of Apollo 12 mare basalts has been examined with emphasis on trace-element ratios and abundances. Vitrophyric basalts were used as parental compositions for the modelling, and proportions of fractionating phases were determined using the MAGFOX program of Longhi (1991). Crystal fractionation processes within crustal and sub-crustal magma chambers are evaluated as a function of pressure. Knowledge of the fractionating phases allows trace-element variations to be considered as either source related or as a product of post-magma-generation processes. For the ilmenite and olivine basalts, trace-element variations are inherited from the source, but the pigeonite basalt data have been interpreted with open-system evolution processes through crustal assimilation. Three groups of basalts have been examined: (1) Pigeonite basalts – produced by the assimilation of lunar crustal material by a parental melt (up to 3% assimilation and 10% crystal fractionation, with an "r" value of 0.3). (2) Ilmenite basalts – produced by variable degrees of partial melting (4–8%) of a source of olivine, pigeonite, augite, and plagioclase, brought together by overturn of the Lunar Magma Ocean (LMO) cumulate pile. After generation, which did not exhaust any of the minerals in the source, these melts experienced closed-system crystal fractionation/accumulation. (3) Olivine basalts – produced by variable degrees of partial melting (5–10%) of a source of olivine, pigeonite, and augite. After generation, again without exhausting any of the minerals in the source, these melts evolved through crystal accumulation. The evolved liquid counterparts of these cumulates have not been sampled. The source compositions for the ilmenite and olivine basalts were calculated by assuming that the vitrophyric compositions were primary and the magmas were produced by non-modal batch melting. Although the magnitude is unclear, evaluation of these source regions indicates that both be composed of early- and late-stage Lunar Magma Ocean (LMO) cumulates, requiring an overturn of the cumulate pile.

INTRODUCTION

Developments in lunar research have highlighted the evolution of Earth's only satellite *via* the crystallization of a Lunar Magma Ocean (LMO) or magmasphere, which led to the formation of the lunar mantle and crust (*e.g.*, Taylor, 1982; Warren, 1985). Mare basalts are derivatives from this cumulate mantle and have been generally classified according to variations in TiO_2 contents (Papike *et al.*, 1976; Papike and Vaniman, 1978) with a more specific classification on the basis of Ti, Al, and K contents (Neal and Taylor, 1992). As no mantle xenoliths have been returned from the Moon, direct knowledge of mantle composition and processes remains elusive. However, the nature of the cumulate mantle and any speculated overturn events can be evaluated by the study of the mare volcanic products.

Experimental petrology suggests that low- and high-Ti mare basalts are derived from different depths within the cumulate mantle (high-Ti = 100-150 km, *e.g.*, Longhi *et al.*, 1974; low-Ti = >200 km, *e.g.*, Kesson, 1975). Therefore, they should possess different Mg#s [100*(Mg/(Mg+Fe))], if the cumulate "layer cake" model for the lunar mantle is correct (*i.e.*, early cumulates at the base of the mantle and later crystallizing phases at the top). However, lunar basalts exhibit similar Mg#s and variations therein (*e.g.*, Papike *et al.*,1976; Neal and Taylor, 1992). Other authors suggested that the high- and low-Ti basalts were derived from similar depths (*e.g.*, Papike *et al.*, 1976), or that the available data could be interpreted in several ways (Longhi, 1992; Shearer and Papike, 1993). Ringwood and Kesson (1976), Hughes *et al.* (1988), Spera (1991, 1992), and Hess (1991, 1993) proposed the mixing of early- and late-stage cumulates and trapped (KREEP-like) liquid by late-stage convective overturn of the cumulate pile or sinking of heavy, late-stage cumulates (*i.e.*, TiO_2-rich). Recently, the scale of this convective overturn has been questioned by Snyder *et al.* (1992), who suggested that such overturn occurred not only on a localized scale but throughout the crystallization of the LMO. If this model is correct, the trapped liquid represents the LMO melt at all stages of evolution (being trapped instantaneously as the cumulates crystallize), and the instability required to cause catastrophic overturn of the cumulate pile is never reached.

This paper uses the Apollo 12 mare basalts as windows into the lunar mantle and is the second in a two part contribution concerning Apollo 12 mare basalt petrogenesis. Part 1 of this contribution (Neal *et al.*, 1994) reported mineralogy, petrography, and whole-rock chemistry for five "new" Apollo 12 basalts (*i.e.*, previously unanalyzed), as well as highlighting: (1) whole-rock chemical data for five previously unanalyzed Apollo 12 mare basalts (three from the ilmenite suite and one each from the pigeonite and olivine basalt suites); (2) unrepresentative sampling problems in five Apollo 12 basalts; (3) the reclassification of two (12031 and 12072) of the three basalts which formed the feldspathic suite, with 12038 remaining as the sole representative of this group; and (4) the fact that the olivine and pigeonite basalts are not co-magmatic. The focus of this paper is to combine this information with existing data in undertaking a detailed examination of the Apollo 12 low-Ti/low-Al/low-K mare basalt compositions in order to define petrogenetic evolution models for each group of basalts present at this site. Emphasis is placed upon trace-element abundances and ratios in order to differentiate signatures inherited from the source with those imparted upon the evolving magma by post-magma-generation processes.

WHOLE-ROCK CHEMICAL DATA

A data base of whole-rock chemical data has been amassed using published analyses (see caption of Fig. 1 for references). Each basalt was evaluated for sample heterogeneity using the three criteria outlined in Neal *et al.* (1994): (1) Petrographic Heterogeneity; (2) Chemical Heterogeneity; and (3) Plotting Consistency. Four basalts are considered to yield whole-rock chemical data which are unrepresentative of the bulk composition (Neal *et al.*, 1994): 12005, an ilmenite basalt; 12006 and 12036, olivine basalts; and 12031, originally described as a feldspathic basalt (Rhodes *et al.*, 1977; Beaty *et al.*, 1979), but reclassified as a plagioclase-rich pigeonite basalt by Nyquist *et al.* (1979). The feldspathic suite is not considered in this study of Apollo 12 mare basalt petrogenesis as it is composed of only one sample, 12038 (Neal *et al.*, 1994).

Averaged data were used where more than one analysis of the same basalt has been reported, and all basalts have been plotted. Average compositions of basalts which have been highlighted as yielding unrepresentative whole-rock analyses generally plot away from the trends exhibited by their respective basalt suites (*e.g.*, Figs. 1–3).

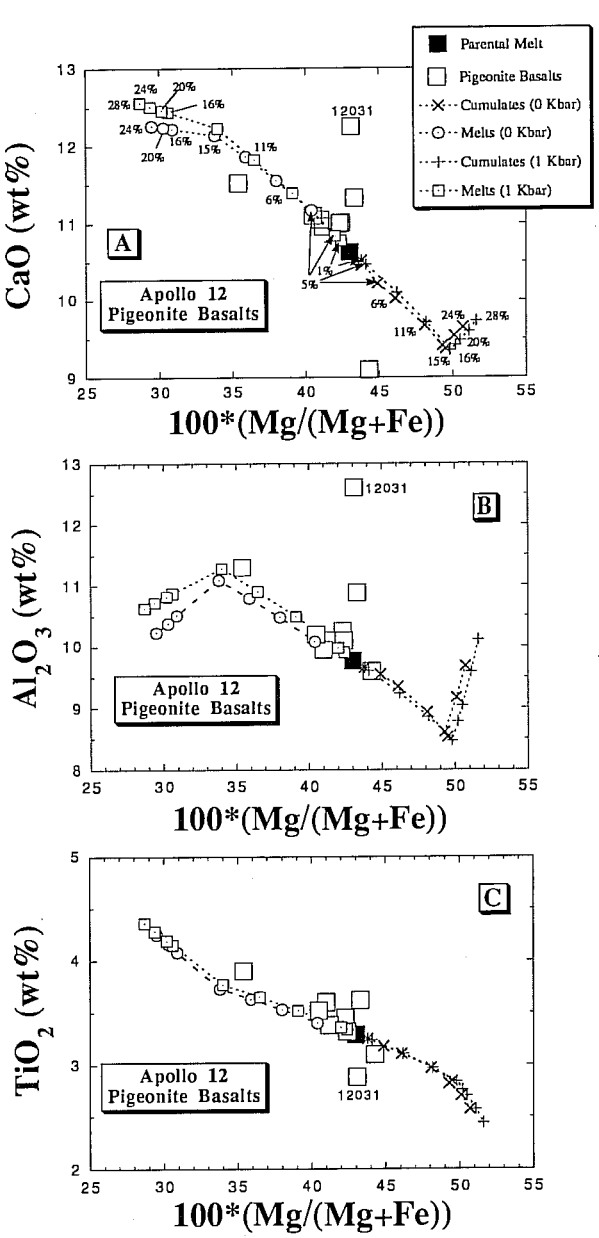

FIG. 1. Major element modelling by closed system crystal fractionation/cumulation of the Apollo 12 pigeonite basalts: (a) 100*[Mg/(Mg+Fe)] *vs.* CaO; (b) 100*[Mg/(Mg+Fe)] *vs.* Al_2O_3; (c) 100*[Mg/(Mg+Fe)] *vs.* TiO_2. Evolution paths generated by the MAGFOX program of Longhi (1991). Data from Beaty *et al.* (1979); Brunfelt *et al.* (1971); Compston *et al.* (1971); Cuttitta *et al.* (1971); Engel *et al.* (1971); Haskin *et al.* (1971); Hubbard and Gast (1971); Kharkar and Turekian (1971); Kushiro and Haramura (1971); LSPET (1970); Maxwell and Wiik (1971); Morrison *et al.* (1971); Neal *et al.* (1994); Nyquist *et al.* (1979); Rhodes *et al.* (1977); Schnetzler and Philpotts (1971); Scoon (1971); Taylor *et al.* (1971); Vobecky *et al.* (1971); Wakita and Schmitt (1971); Wakita *et al.* (1971); Wänke *et al.* (1971); Willis *et al.* (1971).

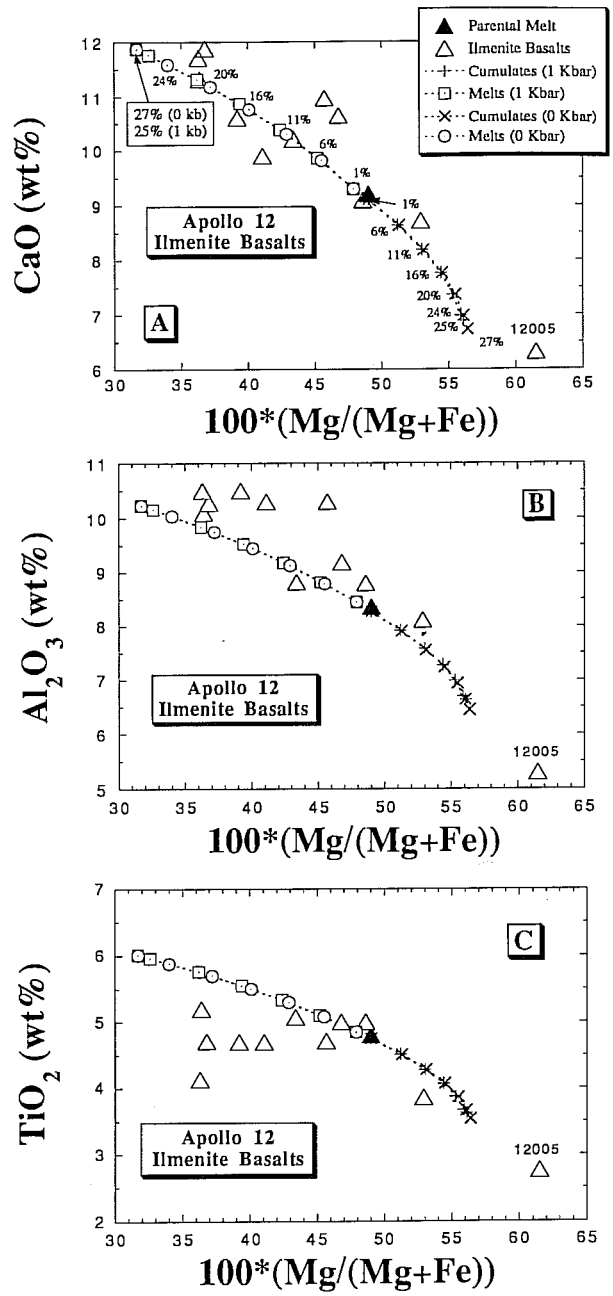

FIG. 2. Major element modelling by closed system crystal fractionation/cumulation of the Apollo 12 ilmenite basalts: (a) 100*[Mg/(Mg+Fe)] *vs.* CaO; (b) 100*[Mg/(Mg+Fe)] *vs.* Al_2O_3; (c) 100*[Mg/(Mg+Fe)] *vs.* TiO_2. Evolution paths generated and data sources the same as in Fig. 1.

DISCUSSION

Crystal Fractionation/Accumulation

The Apollo 12 ilmenite, olivine, and pigeonite basalts have previously been interpreted as having evolved through single-stage, closed-system crystal fractionation/accumulation at low pressure from a parent represented by the vitrophyric samples present in each basalt suite (*e.g.*, Kushiro and Haramura, 1971; James and Wright, 1972; Walker *et al.*, 1976; Dungan and Brown, 1977; Rhodes *et al.*, 1977; Baldridge *et al.*, 1979; Beaty *et al.*, 1979). The olivine and pigeonite basalts were interpreted as being co-magmatic (*e.g.*, James and Wright, 1972), but we have demonstrated that these basalts are unrelated, being independently derived from distinct and separate sources (Neal *et al.*, 1994).

The previous petrogenetic models have been re-evaluated using the MAGFOX program of Longhi (1991). This program allows the proportions and types of fractionating phases to be deduced at varying pressures. Use of this program allows a first

approximation of the processes which could account for the compositional variations in the Apollo 12 mare basalts. The major-element variations in the Apollo 12 pigeonite, ilmenite, and olivine basalt suites have been modelled by crystal fractionation and accumulation of a single parental composition at 1 bar (representing crustal magma chambers) and 1 kbar (approximating crust-mantle boundary magma chambers) and demonstrate inconsistencies with a single-stage crystal-fractionation model. As in previous models, vitrophyre/fine-grained compositions within each group have been taken as representing the parent magma. Furthermore, experimental evidence highlighting crystallization

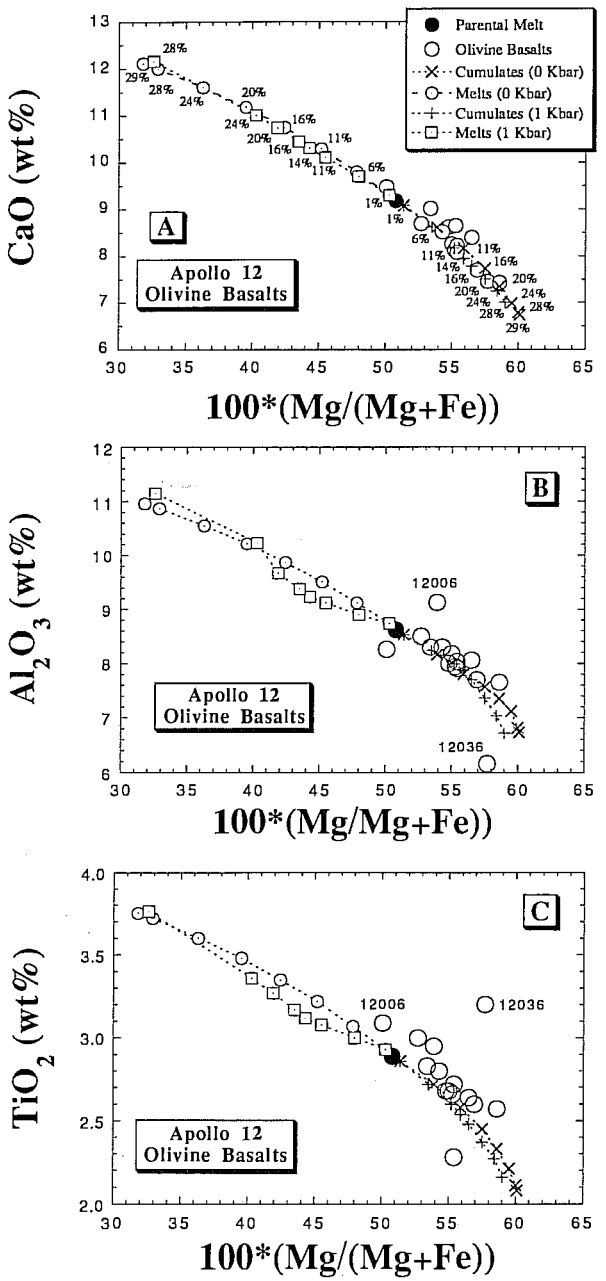

FIG. 3. Major element modelling by closed system crystal fractionation/cumulation of the Apollo 12 olivine basalts: (a) 100*[Mg/(Mg+Fe)] *vs.* CaO; (b) 100*[Mg/(Mg+Fe)] *vs.* Al_2O_3; (c) 100*[Mg/(Mg+Fe)] *vs.* TiO_2. Evolution paths generated and data sources the same as in Fig. 1.

parameters (*e.g.*, Green *et al.*, 1971; Walker *et al.*, 1976) also identifies parental compositions as being represented by the vitrophyres within each suite. Therefore, for this study, the pigeonite basalt parent is taken as vitrophyre 12011; the ilmenite basalt parent is the average of vitrophyre 12008 and fine-grained quenched basalts, 12022 and 12045; and the olivine-basalt parent is the average of two vitrophyres, 12009 and 12015. It was assumed that the amount of glass present in these samples signifies quenching that essentially freezes in the parental composition. Dungan and Brown (1977) argued that ilmenite vitrophyre 12008 may have "experienced a small net gain of olivine at some point", whereas quenched (very fine-grained/glassy) ilmenite basalts 12022 and 12045 experienced 2% and 7% olivine removal, respectively. Therefore, averaging allows the parental composition to be a more acceptable estimate. A similar argument can be made for averaging the compositions of olivine vitrophyres 12009 and 12015 in order to obtain parental or approximate primary compositions.

If the most recent petrogenetic models are correct, the pigeonite basalts (Fig. 1a–c) should all be evolved derivatives of a single parent represented by the vitrophyre 12011 and this is generally the case. However, the vitrophyre 12011 does not contain the highest Mg# (43.0), which may indicate that sample 12019 (Mg# = 44.3) has experienced some crystal accumulation (presence of olivine phenocrysts). Using 12011 as the parental composition, the following fractionating sequence was determined for the pigeonite basalts using the MAGFOX program (Table 1). As Longhi (1987) pointed out, the modelling of chromite crystallization is only approximate using the MAGFOX program, and we interpret it as such here. Therefore, the concentration of any element dominated by chromite fractionation (*e.g.*, Cr) will only be approximated, and we will not include Cr in our petrogenetic modelling for the pigeonite, ilmenite, or olivine basalts.

In our modelling, we used the fractionating assemblages derived from vitrophyre representatives of each of the pigeonite, ilmenite, and olivine basalt suites, using the MAGFOX program (Table 1). The fractionating assemblages identified by the MAGFOX program are consistent with petrographic observations. The ilmenite basalts conform approximately to the calculated liquid line of descent when Mg# is plotted against CaO (Fig. 2a) but not when it is plotted against Al_2O_3 or TiO_2 (Fig. 2b,c). Likewise, while all olivine basalts have been described as cumulates (*e.g.*, James and Wright, 1972) on the basis of petrography and also when Mg# is plotted against Al_2O_3 and CaO, the majority of basalts plot slightly above the calculated trends when plotted against TiO_2 (Fig. 3a–c).

Source Modelling

Modelling of the source region(s) for Apollo 12 mare basalts was undertaken by Ma *et al.* (1976), as part of a study of chemical constraints for mare basalt genesis. Ma *et al.* (1976) observed no significant La/Sm-La and Sm/Eu-La correlations within the Apollo 12 basalt suite as a whole. The La/Sm and La ranges of most Apollo 12 basalts coincide approximately with the chemically similar Apollo 15 mare basalts, indicating similar heterogeneous source materials and mechanisms for their genesis (Ma *et al.*, 1976). These authors further suggested that the narrow range of Sm/Eu and weak Sm/Eu *vs.* La correlation may be due to a lack of plagioclase in the source.

Shih and Schonfeld (1976) reported the results of a study of high- and low-Ti mare basalt sources, which were calculated from

observed basaltic compositions and radiogenic isotope data. These authors concluded that Apollo 12 and 15 basalts were derived by a small degree of partial melting of a cumulate source comprised of mainly olivine, clinopyroxene, and orthopyroxene, with minor plagioclase or spinel at greater depths. Extending this Apollo 12 mare basalt source modelling, Nyquist *et al.* (1977, 1979, 1981) concluded that multiple sources were required in order to generate the observed compositional groups of Apollo 12 basalts. Essentially, the conclusions are the same as Shih and Schonfeld (1976) in that the isotopic and REE compositions of the Apollo 12 basalts can be generated by small (2–10%) degrees of partial melting of cumulate sources composed of varying proportions of olivine, orthopyroxene, and clinopyroxene. An important feature of this model is that non-chondritic relative abundances of the REE must be assumed in the parental magma ocean at the time of cumulate source formation.

Trace-element ratios can yield information regarding source composition and post-magma-generation processes. As noted above, the involvement of plagioclase in the source region of the Apollo 12 low-Ti mare basalts has been the subject of some debate (*e.g.*, Ma *et al.*, 1976; Shih and Schonfeld, 1976; Nyquist *et al.*, 1977, 1979, 1981). Therefore, the trace-element contents are discussed in terms element-element ratios as well as abundances. The ratios allow an evaluation of fractionation/accumulation (Co/Hf), and the effects of the presence of pyroxene (Sc/Sm), clinopyroxene (Rb/Sr), and plagioclase (Sm/Eu and Rb/Sr), either in the source or in the fractionating assemblage. We have demonstrated that the pigeonite, ilmenite, and olivine basalt suites are not related (Neal *et al.*, 1994). One immediate result of our modelling is that the compositional variation exhibited by each of the three individual Apollo 12 mare basalt suites cannot be generated from a single parental magma by closed-system crystal fractionation/accumulation. Error bars on subsequent diagrams have been calculated through consideration of the variations in the trace-element ratios for several analyses of the same basalt. The ranges in these trace-element ratios displayed by each mare basalt suite are generally greater than that of the calculated error. Those samples which have been analyzed more than once were compared and those exhibiting marked differences were described as "unrepresentative". However, basalts analyzed more than once and having similar compositions with each analysis indicate that unmixing is not a problem. We assume that the analysis of those basalts analyzed only once is representative. Therefore, the range in those element-element ratios which are not affected by fractional crystallization in these cases (*i.e.*, Sm/Eu and Rb/Sr) must be inherited from the source through variable degrees of partial melting, or from open-system behavior.

Apollo 12 Mare Basalt Petrogenesis

Pigeonite Basalts–Early petrogenetic models suggested that the pigeonite basalts were the evolved counterparts of the olivine basalts (*i.e.*, James and Wright, 1972). Rhodes *et al.* (1977) concluded that the olivine and pigeonite basalts were co-magmatic, but we have demonstrated in Part 1 (Neal *et al.*, 1994) that these two basaltic groups are distinct and unrelated, using Co/Sm, Sm/Eu, and Rb/Sr variations which exceeded those expected from fractional crystallization. Major-element correlations suggest that generally all pigeonite basalts are evolved melts derived from a parent represented by vitrophyre 12011 (Fig. 1a–c), consistent with previous models of closed-system crystal fractionation. These

TABLE 1. Modelling parameters.
A. Partition Coefficients.

	Olivine	Spinel	OPX	Pigeonite	CPX	Plagioclase	Ilmenite
Sc	0.27	0.048	1.6	1.6	1.6	0.0071	1.5
Cr	3	15	5	5	5	0.0332	4.2
Co	5	1	1.3	1.3	1.2	0.0202	4.3
Ce	0.0001	0.009	0.009	0.00172	0.039	0.302	0.0019
Sm	0.0006	0.006	0.022	0.011	0.17	0.017	0.0023
Eu	0.0007	0.006	0.015	0.0068	0.16	1.2	0.0009
Yb	0.019	0.008	0.17	0.087	0.29	0.0065	0.057
Hf	0.013	0.085	0.063	0.063	0.063	0.0128	0.406
Rb	0.0001	0.001	0.023	0.0026	0.015	0.08	0.001
Sr	0.0001	0.001	0.018	0.002	0.116	1.61	0.001

Data taken from partition coefficients compiled by Snyder *et al.* (1992) and references therein for lunar applications, except for spinel data which was taken from Neal *et al.* (1988).

B. Vitrophyre/parental melt compositions used in modelling.

	Olivine	Ilmenite	Pigeonite
SiO_2 (wt%)	45.01	42.75	46.63
TiO_2	2.89	4.80	3.29
Al_2O_3	8.62	8.36	9.77
Cr_2O_3	0.62	0.59	0.59
FeO	20.57	21.82	19.53
MnO	0.28	0.28	0.29
MgO	11.91	11.46	8.26
CaO	9.18	9.21	10.63
Na_2O	0.23	0.33	0.25
Mg#	50.8	48.3	43.0
Sc (ppm)	46.7	53.8	52.2
Co	49.3	50.3	39.0
Ce	16.6	16.4	19.9
Nd	14.8	16.0	15.0
Sm	4.43	5.55	5.00
Eu	0.945	1.26	0.95
Yb	3.75	5.19	4.20
Hf	3.7	4.5	3.7
Rb	1.124	0.729	1.220
Sr	96.86	136.9	112.7

C. Fractionating phases from parental compositions.

% Cryst.	Olivine	Cr-Spinel	Pigeonite	Plag.	Cpx
Pigeonite Basalts					
0-1	100	----	----	----	----
1-5	80	20	----	----	----
5-15	----	2	98	----	----
15-30	----	----	33	67	----
Olivine Basalts					
SOURCE	**48**	----	**22**	----	**30**
0-1	100	----	----	----	----
1-23	94	6	----	----	----
23-30	----	----	100	----	----
Ilmenite Basalts					
SOURCE	**45.5**	----	**42.5**	**0.5**	**11.5**
0-1	100	----	----	----	----
1-27	94	6	----	----	----
27-28	----	----	100	----	----
28-30	----	----	----	58	42

models (at both 1 bar and 1 kbar) indicate the presence of plagioclase in the crystallizing sequence after 15% fractionation (Fig. 1a–c), with the fractionating sequences being similar at each pressure.

Petrogenetic modelling of the pigeonite basalts must account for the correlation between Al_2O_3 and Co (Fig. 4a) and the decrease in Sm/Eu and Rb/Sr ratio from the parent 12011 (Fig. 4b). With closed-system crystal fractionation, the onset of plagioclase crystallization restricts the increase of Al_2O_3 in the residual melt (Fig. 4a inset). Cobalt decreases in the residual melt until olivine and chromite-ulvöspinel cease crystallizing, then it becomes incompatible (Fig. 4a), but the magnitude of the Co decrease during crystal fractionation never attains the range of Co concentrations displayed by the pigeonite basalt suite. The Al_2O_3 increases then decreases once plagioclase becomes a liquidus phase (Fig. 4a). The failure of closed-system crystal fractionation to account for the petrogenesis of the pigeonite basalts is dramatically displayed in Fig. 4b. Here, the Sm/Eu and Rb/Sr ratios of the pigeonite basalts decrease from the parental composition, but the calculated crystal fractionation path shows that residual magmas from the parent would exhibit increases in both these ratios. Therefore, compositional variations exhibited by the pigeonite basalts cannot be accounted for by closed-system crystal fractionation. The compositional variations exhibited by the pigeonite basalts were also modelled by variable degrees of partial melting of a source calculated from parental basalt 12011. This approach also failed to account for the compositional ranges even if plagioclase was present in the source.

The process of crustal assimilation was explored, as this can significantly increase the Al_2O_3 content of the residual magma beyond that of simple crystal fractionation. The composition of any crustal assimilant is non-unique, because of the heterogeneity that exists within the lunar crust. Possible crustal contaminant compositions were evaluated from pristine highlands compositions from the Apollo 12 and 14 sites (Warren *et al.*, 1983, 1990; Lindstrom *et al.*, 1984; Shervais *et al.*, 1984; Goodrich *et al.*, 1986;

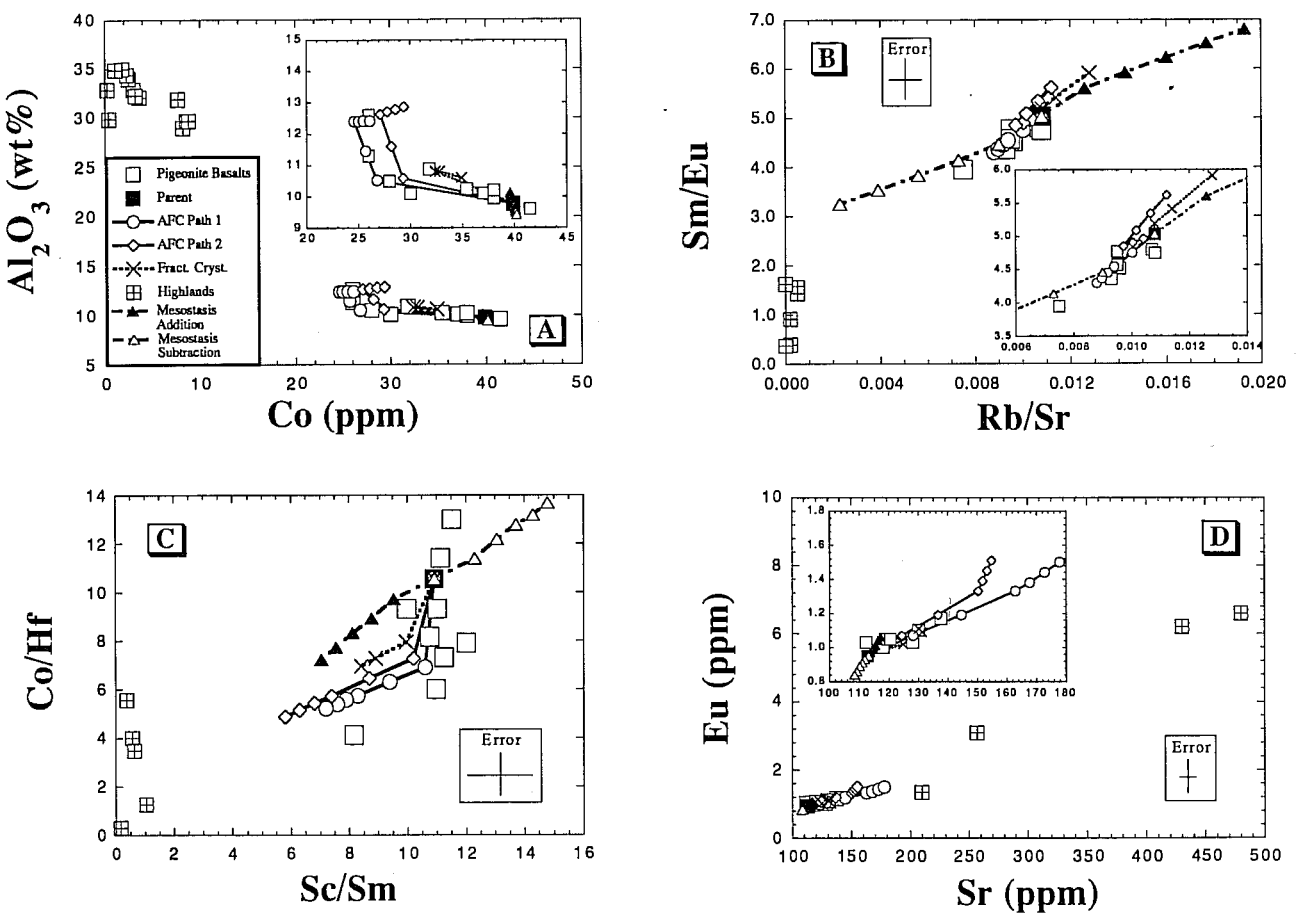

FIG. 4. Petrogenetic model for the Apollo 12 pigeonite basalts *via* assimilation of anorthositic lunar crust using the compositions in Table 2. Pigeonite basalt data sources are as in Fig. 1. The AFC paths have been calculated using end-member anorthositic lunar crustal compositions from Warren *et al.* (1983, 1990); Lindstrom *et al.* (1984); Shervais *et al.* (1984); Goodrich *et al.* (1986); Neal *et al.* (1991); Snyder *et al.* (pers. comm.,1993) and an "r" value of 0.3. Each AFC path is plotted in increments of 5% FC. The closed-system FC paths are plotted in increments of 10% crystallization. Fractionating phases for FC and AFC paths are as in Table 1. Also plotted are paths depicting the effects of short-range unmixing *via* mesostasis migration (addition/subtraction). Each path is calculated for 5% mesostasis addition/subtraction, in 1% increments, from the parental composition. (A) Al_2O_3 (wt%) *vs.* Co (ppm). The inset highlights the pigeonite basalt compositions and the AFC and FC paths. Both AFC trends follow the same path, but the FC path exhibits a reversal after 10%. (B) Sm/Eu *vs.* Rb/Sr. All Rb/Sr data are by isotope dilution. The basalts require assimilation of anorthositic lunar crust in order to account for their compositions, as the FC path trends in the opposite direction to the data. The maximum extent of AFC path 1 is 15% FC (4% assimilation). Greater amounts of AFC produce a reversal of the path, back toward the parental compositions, because of the influence of plagioclase crystallization. (C) Co/Hf *vs.* Sc/Sm. (D) Sr (ppm) *vs.* Eu (ppm). The inset highlights the pigeonite basalt compositions and demonstrates that these basalts are not generated by 30% FC, but are by <10% AFC with anorthositic lunar crust.

Neal *et al.*, 1991; Snyder *et al.*, pers. comm., 1993). These have been plotted with the pigeonite basalt data and demonstrate the heterogeneity of the lunar crust in this area (Mg-Suite, Alkali Suite, and rare FANs). However, if crustal assimilation produced the compositional ranges displayed by the pigeonite basalts, the contaminant must have been Al-, Sr-, and Eu-rich (anorthositic) (Fig. 4a,d), with low Sm/Eu and Rb/Sr ratios (Fig. 4b), and REE-poor (Fig. 4c).

The details of lunar crustal assimilation have been studied by Finilla *et al.* (1993, 1994) using thermodynamic reasoning and simple fluid mechanical constraints. These authors suggested that the maximum amount of crustal assimilation possible in a rigorously convecting magma was 6%. The work of Finnila *et al.* (1993, 1994) assumed a noritic to troctolitic crustal composition, the assimilation of which would change the Al_2O_3 content by 0.9 wt%. Clearly, if anorthositic crust was assimilated, the Al contribution from the assimilant increases. If the magma was non-convecting, then assimilation proceeds by the slower process of dissolution, which is too slow to significantly affect the magma composition (Finilla *et al.*, 1993a,b). Warren (1986) reported anorthosite assimilation models which could lead to an "r" value around 0.3 (r = mass assimilated/mass crystallized = 0.3). Using these constraints, the petrogenesis of the pigeonite basalts has been modelled by AFC (DePaolo, 1981) of a convecting parental magma assimilating heterogeneous anorthositic lunar crust. Rather than a path, an "AFC band" has been calculated using end members (Table 2) of the anorthositic highlands samples depicted in Fig. 4a–d, the fractionating assemblage determined by the MAGFOX program (Table 1), and partition coefficients applicable to lunar systems compiled by Snyder *et al.* (1992) and references therein (Table 1). Results of the AFC model are also presented in Table 2 and suggest that the pigeonite basalt compositions were generated in a crustal rather than a mantle magma chamber.

Generally, the pigeonite basalts can be generated with < 3% assimilation or < 10% crystallization. The exception to this is the original feldspathic basalt 12031, but we note here that it does not plot in a consistent way along the model AFC band in Fig. 4a–d and have argued that the reported analysis is unrepresentative of the whole-rock composition (Neal *et al.*, 1994). While the AFC band shows a decrease followed by an increase in Co and an increase followed by a decrease in Al_2O_3 (similar to the crystal fractionation path, Fig. 4a), the compositional range displayed by the pigeonite basalts has been successfully modelled. The AFC band in Fig. 4b reflects the concentrations of Eu and Sr in the assimilant compositions. While the crystal fractionation path follows the basalt data when Co/Hf is plotted against Sc/Sm (Fig. 4c), the model path exhibits less dramatic decreases in Co/Hf and Sc/Sm ratios compared to the AFC paths. Strontium and Eu abundances can be successfully modelled by a maximum of 3% assimilation coupled with 10% crystal fractionation, whereas 30% closed-system crystal fractionation would be required (Fig. 4d).

The Sr isotope data should be able to distinguish between source heterogeneity and open system behavior. Neodymium isotope data for the three pigeonite basalts reported by Nyquist *et al.* (1979) and Unruh *et al.* (1984) (12011, 12031, and 12039) suggest closed-system processes [$(\epsilon_{Nd})_I$ = +5.0 to +5.4)]. When initial Sr isotope ratios are considered, it is evident that there is variation in I(Sr) outside analytical error (Fig. 5). The calculated AFC paths exhibit a reversal due to the onset of plagioclase crystallization (Fig. 5). Variation in I(Sr) is not a simple progression from a relatively radiogenic $^{87}Sr/^{86}Sr$ ratio of the parent to the relatively non-radiogenic anorthositic crustal signature of the most evolved end member (*i.e.*, the progression expected for a magma assimilating plagioclase-rich crust which has a low Rb/Sr ratio and hence an unradiogenic $^{87}Sr/^{86}Sr$ signature) (Fig. 5). This is at variance with the trace-element modelling presented above, but if the crust being assimilated is ancient and heterogeneous with respect to Rb/Sr ratio, the isotopic ratios will be more sensitive to this heterogeneity, especially as the Sr contents of the crust ranges from 2–4x that of the parental magma. However, the modelling of the isotopic ratios is severely restricted by the lack of age and initial ratio data of anorthositic crust from the western region of the Moon. For our modelling purposes, the data of the Mg-Suite anorthosite 14303,347 (Snyder *et al.*, pers. comm., 1993) was used: Rb = 0.494 ppm; Sr = 257 ppm; I(Sr) = 0.69915. The same initial ratio was used to calculate both AFC paths (Fig. 5), but the Rb and Sr contents were varied to account for the variable nature of the lunar crust (see Table 2). Clearly, while the major- and trace-element data suggest a simple AFC process can account for the petrogenesis of the pigeonite basalts, the Sr isotope data suggest

TABLE 2. AFC model for the petrogenesis of Apollo 12 pigeonite mare basalts. Results are in ppm

	Sc	Co	Ce	Sm	Eu	Yb	Hf	Rb	Sr	Rb/Sr	Sm/Eu	Sc/Sm	Co/Hf	$^{87}Sr/^{86}Sr$
PIGEONITE BASALTS														
PARENT	52.2	39	18.5	4.78	0.920	3.93	3.70	1.220	112.7	0.0108	5.03	10.9	1094	0.69954
ASSIM.[1]	0.36	0.25	10.0	1.88	3.03	0.89	0.12	0.100	430	0.0002	0.62	0.19	193	0.69915
5% AFC[1]	54.0	26.8	19.7	5.07	1.07	4.15	3.89	1.286	128.2	0.01003	4.75	10.6	6.90	0.69951
10% AFC[1]	50.7	25.7	20.9	5.38	1.19	4.36	4.08	1.36	144.6	0.00937	4.51	9.4	6.30	0.69949
15% AFC[1]	47.4	24.6	22.3	5.71	1.33	4.59	4.29	1.43	162.9	0.00880	4.30	8.3	5.73	0.69946
20% AFC[1]	48.0	25.0	23.7	6.05	1.38	4.84	4.50	1.50	167.7	0.00897	4.37	7.9	5.56	0.69944
25% AFC[1]	48.6	25.5	25.2	6.42	1.44	5.12	4.75	1.58	172.7	0.00917	4.45	7.6	5.38	0.69943
30% AFC[1]	49.3	26.1	26.9	6.84	1.50	5.43	5.02	1.67	177.8	0.00940	4.55	7.2	5.20	0.69941
ASSIM.[2]	2.3	8.2	77.2	12.2	3.09	6.68	6.57	0.494	257	0.0019	3.95	0.19	26.2	0.69915
5% AFC[2]	54.0	29.3	21.2	5.30	1.07	4.28	4.03	1.295	124.3	0.01041	4.96	10.2	7.26	0.69952
10% AFC[2]	50.8	28.2	24.0	5.85	1.19	4.63	4.37	1.370	136.6	0.01005	4.90	8.7	6.45	0.69951
15% AFC[2]	47.5	27.1	27.2	6.46	1.33	5.01	4.75	1.46	150.3	0.00972	4.85	7.4	5.71	0.69949
20% AFC[2]	48.2	27.8	30.3	7.07	1.39	5.41	5.14	1.54	151.8	0.01017	5.08	6.8	5.42	0.69948
25% AFC[2]	48.8	28.6	33.8	7.74	1.45	5.86	5.57	1.63	153.3	0.01066	5.34	6.3	5.14	0.69946
30% AFC[2]	49.6	29.4	37.7	8.50	1.51	6.35	6.05	1.73	154.8	0.01121	5.62	5.8	4.86	0.69945

1 = AFC Path 1; 2 = AFC Path 2; ASSIM. = Assimilant Composition.

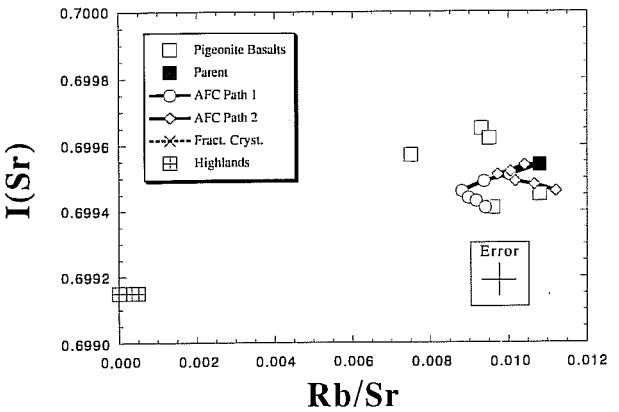

FIG. 5. I(Sr) *vs.* Rb/Sr. The FC path plots directly on top of the parental composition as neither I(Sr) or Rb/Sr change. Basalt data from Bottino *et al.* (1971); Compston *et al.* (1971); Murthy *et al.* (1971); Nyquist *et al.* (1977, 1979); Papanastassiou and Wasserburg (1970, 1971). Assimilant data from Snyder *et al.* (pers. comm., 1993) and Neal *et al.* (1991).

that this process was complicated by the heterogeneous nature of the assimilated crust.

Ilmenite Basalts–Dungan and Brown (1977) concluded that the ilmenite suite was comprised of both evolved and cumulate end-members. As stated above, we have used an average of three vitrophyric/quench-textured ilmenite basalts as the parental composition, in order to remove the effect of slight olivine removal/accumulation in individual samples (Dungan and Brown, 1977). The MAGFOX program indicates that there is no difference in the fractionating assemblage of this parental composition at 1 bar and 1 kbar, just a slight difference in the timing of each mineral becoming a liquidus phase. A limit of 30% crystal fractionation/accumulation was arbitrarily imposed as the bulk of the ilmenite basalt major-element data appeared to be satisfied by this percentage (Fig. 2). Plagioclase does not become a liquidus phase until >27% crystallization and as noted above, cannot account for the range in Sm/Eu or Rb/Sr ratios unless fractional crystallization is >50%. Clearly, such a high percentage of crystallization is inconsistent with the major elements (Fig. 2).

The petrogenetic model developed here assumes that the parental melt is a primary composition. It is used to calculate a source composition for the ilmenite basalts, similar to the method of Nyquist *et al.* (1977), but using a non-modal batch melting approach:

$$C_s = C_l / [1/(D + F(1-P))]$$

where C_s = Elemental concentration in source; C_l = Elemental concentration in the parent; D = Bulk distribution coefficient calculated from source mineralogy; F = Amount of partial melt; P = Distribution coefficient calculated from mode going into the melt.

Partition coefficients used in this study have generally been determined for lunar applications (Snyder *et al.*, 1992 and references therein. Those applicable for this study are given in Table 1). Initially, it was assumed that the parent was a 6% partial melt of a source comprised of 38% clinopyroxene + 31% orthopyroxene + 31% olivine, as calculated by Nyquist *et al.* (1977, 1979). However, the range in Sm/Eu and Rb/Sr ratios cannot be derived from a single parental melt (followed by closed-system crystal fractionation/accumulation) generated by the parameters defined by Nyquist *et al.* (1979). Therefore, after deriving a source composition and assuming the mineralogy of Nyquist *et al.* (1977, 1979), we calculated melt compositions at 2%, 4%, 6%, and 8% partial melting. However, the path generated did not conform to the data array. In order that the data can be modelled by this method, the parental composition (Table 1) is required to be a 6% partial melt of a source composed of 45.5% olivine + 42.5% pigeonite + 11.5% clinopyroxene + 0.5% plagioclase melting in the proportions of 1.5:4.5:3.5:0.5. Plagioclase is exhausted after 10% partial melting is exceeded. This source assumes a significant ilmenite component (3%) dissolved in the clinopyroxene and is similar to that proposed by Snyder *et al.* (1992) for Ti-rich mare basalts, except that no trapped liquid or ilmenite is required to generate the melt path depicted in Fig. 6a. In order to generate variable Rb/Sr ratios at relatively constant Sm/Eu, modelling of 2%, 4%, 6%, and 8% partial melting of this source appears to generate all basalt compositions (Fig. 6a and Table 3). Crystal fractionation will not alter the Sm/Eu and Rb/Sr ratios until plagioclase becomes a liquidus phase (>27% crystallization). The fractionation sequence defined for the vitrophyric samples was applied to each of the model partial melts. Such variations in partial melting will cause differences in TiO_2 contents of the melts generated of up to ≈0.5 wt%. In the three vitrophyric/fine grained ilmenite basalts, such a variation in TiO_2 is seen (12008 = 4.45 wt%; 12022 = 5.16 wt%; 12045 = 4.78 wt%). Could these three represent distinct melting events rather than olivine removal/accumulation? The presence of early (olivine) and late-stage cumulates (augite + ilmenite) in the ilmenite basalt source can be achieved by overturn of the LMO cumulate pile, but the scale of this overturn is beyond the scope of this paper.

Application of this model to the Co/Hf and Sc/Sm ratios (Fig. 6b) demonstrates its suitability to the petrogenesis of the Apollo 12 ilmenite basalts. The distribution of basalts on either side of the melt generation path (*i.e.*, "cumulates" and "fractionates") is consistent with the observations of Dungan and Brown (1977) in that the majority are evolved liquid compositions (fractionates) rather than cumulates. Note also that all but one of the ilmenite basalts are generated by <25% crystal fractionation/accumulation. This is significant because plagioclase is not on the liquidus, and therefore, all variations in Rb/Sr and Sm/Eu must be either source related or a result of open-system behavior. The cumulate which does not fall on the modelling trend is 12005, but we have argued that the analysis of this basalt is unrepresentative (Neal *et al.*, 1994). A similar scenario is seen when trace-element abundances are plotted (Fig. 6c). A major conclusion of this model is that the ilmenite basalts were derived from several parental magmas generated by between 2% and 8% partial melting (Table 3).

Consideration of the initial Sr and Nd isotope ratios of the Apollo 12 ilmenite basalts (Bottino *et al.*, 1971; Compston *et al.*, 1971; Murthy *et al.*, 1971; Nyquist *et al.*, 1977, 1979; Papanastassiou and Wasserburg, 1970, 1971; Unruh *et al.*, 1984) allows an evaluation of open system behavior in order to differentiate between this and source influences. Initial ratios were calculated using both isochron and ^{40}Ar-^{39}Ar ages (*e.g.*, Alexander *et al.*, 1972; Stettler *et al.*, 1973). The bulk Moon evolution path was calculated from BABI using an $^{87}Rb/^{86}Sr$ ratio of 0.04 (Nyquist, 1977), and from the Juvinas eucrite using a $^{147}Sm/^{144}Nd$ ratio of 0.1936 (Lugmair, 1974; Lugmair *et al.*, 1976) (Fig. 6d,e). The ilmenite source evolution path was generated from the Rb/Sr and Sm/Nd ratios calculated during trace-element source modelling in conjunction with the present day $^{87}Sr/^{86}Sr$ and $^{143}Nd/^{144}Nd$ ratios

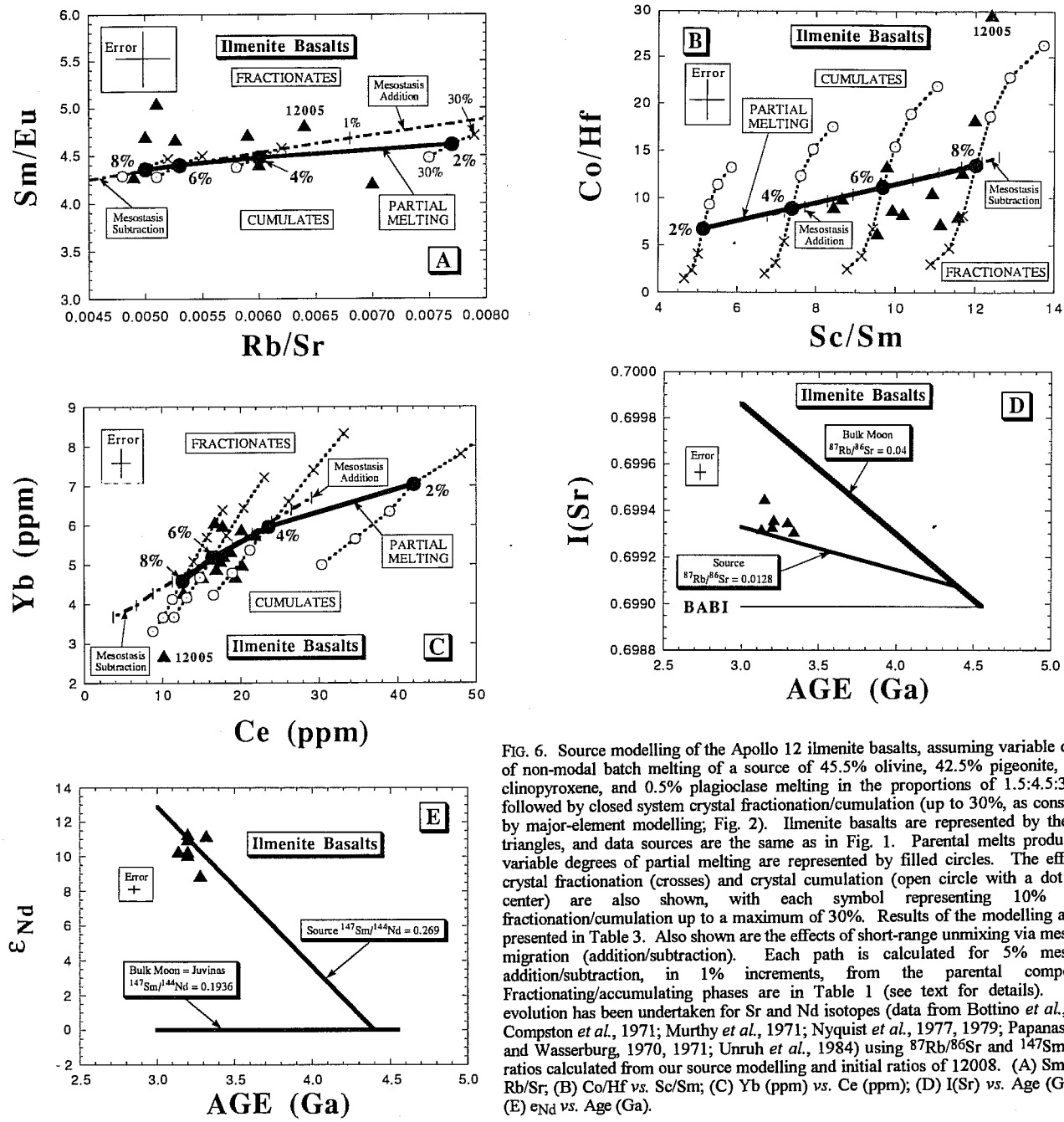

FIG. 6. Source modelling of the Apollo 12 ilmenite basalts, assuming variable degrees of non-modal batch melting of a source of 45.5% olivine, 42.5% pigeonite, 11.5% clinopyroxene, and 0.5% plagioclase melting in the proportions of 1.5:4.5:3.5:0.5, followed by closed system crystal fractionation/cumulation (up to 30%, as constrained by major-element modelling; Fig. 2). Ilmenite basalts are represented by the filled triangles, and data sources are the same as in Fig. 1. Parental melts produced by variable degrees of partial melting are represented by filled circles. The effects of crystal fractionation (crosses) and crystal cumulation (open circle with a dot in the center) are also shown, with each symbol representing 10% crystal fractionation/cumulation up to a maximum of 30%. Results of the modelling are also presented in Table 3. Also shown are the effects of short-range unmixing via mesostasis migration (addition/subtraction). Each path is calculated for 5% mesostasis addition/subtraction, in 1% increments, from the parental composition. Fractionating/accumulating phases are in Table 1 (see text for details). Source evolution has been undertaken for Sr and Nd isotopes (data from Bottino *et al.*, 1971; Compston *et al.*, 1971; Murthy *et al.*, 1971; Nyquist *et al.*, 1977, 1979; Papanastassiou and Wasserburg, 1970, 1971; Unruh *et al.*, 1984) using $^{87}Rb/^{86}Sr$ and $^{147}Sm/^{144}Nd$ ratios calculated from our source modelling and initial ratios of 12008. (A) Sm/Eu *vs.* Rb/Sr; (B) Co/Hf *vs.* Sc/Sm; (C) Yb (ppm) *vs.* Ce (ppm); (D) I(Sr) *vs.* Age (Ga); and (E) ε_{Nd} *vs.* Age (Ga).

of vitrophyre 12008 (Nyquist *et al.*, 1977). The evolution of the Sr isotopes in the source region is documented in Fig. 6d. Generally, the ilmenite basalts plot within error of each other and the calculated evolution path, although slightly above it. Two factors that may account for the source evolution path being lower than the basalts in Fig. 6d are: (1) the assumption that the source departed from the bulk Moon evolution path at 4.4 Ga (*e.g.*, Nyquist *et al.*, 1977, 1979; Nyquist and Shih, 1992 and references therein); and (2) partition coefficients for Sr and especially Rb are not well constrained. The evolution of Nd isotopes in the calculated source demonstrates that source evolution can account for the variations in $^{143}Nd/^{144}Nd$ of the seven basalts reported by Nyquist *et al.* (1979) and Unruh *et al.* (1984). Ilmenite basalt 12051 plots below the array but has a large error associated with this "average" age (Fig. 6e). The extremes reported for 12051 are 3.58 ± 0.3 Ga (Compston *et al.*, 1971) and 3.16 ± 0.04 Ga (Nyquist *et al.*, 1977). Generally, the Sr and Nd isotopes do not indicate open system processes in the petrogenesis of the Apollo 12 ilmenite basalts, suggesting that the variations in incompatible trace-element ratios are inherited from the source. The above model quantifies the nature of the variations in trace-element abundances and ratios observed within the mare basalt suite and demonstrates that they are inherited from the source and/or have been modified by closed-system crystal fractionation/accumulation.

Olivine Basalts–A similar approach to that for the ilmenite basalts was used to develop a petrogenetic model for the Apollo 12

olivine basalts. Again, the MAGFOX program demonstrates that there is little variation in the fractionating assemblage between 1 bar and 1 kbar. Note that neither plagioclase nor Ca-rich clinopyroxene is a liquidus phase and as such, crystal fractionation/accumulation cannot produce the observed ranges in Sm/Eu and Rb/Sr (Fig. 7a), which are outside the calculated error bars. Therefore, these signatures are either inherited from the source or incorporated during open-system evolution.

Hughes *et al.* (1988) conducted source modelling of the Apollo 12 olivine basalts using a hybrid (convective overturn) cumulate source model, where the minerals considered to be representative of early- and late-stage LMO crystallization products were all present in the source. The trapped residual liquid is KREEP-like in composition and is considered to be produced after 99% crystallization of the LMO. Constraints on Apollo 12 olivine basalt source regions, in light of Sm/Nd evolution (Nyquist *et al.*, 1979), show that significant LREE fractionation occurred at the time of magma generation. This assures that models assuming orthopyroxene-free residuals are inadequate to predict a potential source composition, and generates Apollo 12 olivine basalts by between 4% and 12% partial melting of the model source. However, the modelling undertaken by Hughes *et al.* (1988) was upon an average olivine basalt composition. As was demonstrated by Walker *et al.* (1976), many of the Apollo 12 olivine basalts have accumulated olivine by crystal settling and do not represent liquid compositions.

In our model, the parental composition was at first assumed to have been derived by a 3% partial melt of a source composed of 93% olivine and 7% clinopyroxene (after Nyquist *et al.*, 1977). However, this source, even with variable degrees of partial melting will not generate the observed trace-element compositions. Using a similar approach as for the ilmenite basalts, our model requires that the parental composition be the product of 7% non-modal equilibrium partial melting of a source composed of 48% olivine, 22% pigeonite, and 30% clinopyroxene, melting in the proportions 2.5:2.5:5 (Table 2). Unlike the source proposed by Hughes *et al.*

TABLE 3. Trace-element petrogenetic modelling of the Apollo 12 ilmenite basalts *via* different degrees of partial melting followed by closed-system crystal fractionation/accumulation. Results are in ppm.

	Sc	Co	Ce	Sm	Eu	Yb	Hf	Rb	Sr	Rb/Sr	Sm/Eu	Sc/Sm	Co/Hf
ILMENITE BASALTS													
Source Composition													
(6%)	52.1	146.9	1.06	0.45	0.10	0.68	0.44	0.046	10.3	0.0044	4.42	116.3	337
Parental Melts													
2%	53.1	49.8	42.1	10.3	2.24	7.04	7.39	1.980	256.1	0.0077	4.62	5.13	6.73
4%	53.4	50.0	23.6	7.22	1.61	5.97	5.59	1.066	178.4	0.0060	4.48	7.40	8.94
6%	53.8	50.3	16.4	5.55	1.26	5.19	4.50	0.729	136.9	0.0053	4.41	9.69	11.2
8%	54.2	50.6	12.6	4.51	1.03	4.59	3.76	0.554	111.1	0.0050	4.36	12.0	13.4
Fractionates of the 2% Partial Melt													
10%	57.4	33.6	46.7	11.5	2.49	7.80	8.19	2.20	284.3	0.0077	4.62	5.00	4.10
20%	62.6	21.7	52.5	12.9	2.79	8.74	9.18	2.47	319.4	0.0077	4.62	4.85	2.36
30%	67.6	15.6	59.2	14.5	3.08	9.81	10.3	2.78	349.9	0.0079	4.71	4.66	1.51
Cumulates of the 2% Partial Melt													
10%	49.3	62.2	37.9	9.31	2.02	6.35	6.66	1.78	230.5	0.0077	4.62	5.29	9.33
20%	45.5	67.9	33.7	8.27	1.79	5.66	5.94	1.58	204.9	0.0077	4.62	5.50	11.4
30%	42.5	69.1	29.5	7.27	1.62	5.00	5.22	1.39	186.8	0.0075	4.48	5.85	13.2
Fractionates of the 4% Partial Melt													
10%	57.7	33.7	26.2	8.01	1.79	6.61	6.19	1.18	198.0	0.0060	4.48	7.20	5.44
20%	62.9	21.7	29.4	9.00	2.01	7.41	6.94	1.33	222.5	0.0060	4.48	6.99	3.13
30%	68.0	15.7	33.2	10.1	2.21	8.32	7.82	1.50	243.7	0.0061	4.58	6.71	2.01
Cumulates of the 4% Partial Melt													
10%	49.5	62.4	21.2	6.50	1.45	5.38	5.04	0.96	160.6	0.0060	4.48	7.62	12.4
20%	45.8	68.2	18.9	5.78	1.29	4.80	4.49	0.85	142.7	0.0060	4.48	7.93	15.2
30%	42.7	69.4	16.5	5.07	1.16	4.24	3.95	0.75	130.1	0.0058	4.36	8.42	17.6
Fractionates of the 6% Partial Melt													
10%	58.1	33.9	18.2	6.16	1.40	5.75	4.99	0.81	152.0	0.0053	4.4	9.44	6.80
20%	63.4	21.9	20.4	6.92	1.57	6.45	5.59	0.91	170.7	0.0053	4.40	9.16	3.91
30%	68.5	15.8	23.1	7.79	1.73	7.23	6.29	1.02	187.0	0.0055	4.50	8.79	2.51
Cumulates of the 6% Partial Melt													
10%	49.9	62.8	14.8	2.00	1.13	4.68	4.06	0.66	123.2	0.0053	4.40	9.99	15.5
20%	46.1	58.6	13.1	4.44	1.01	4.17	3.62	0.58	109.5	0.0053	4.4	10.4	19.0
30%	43.1	69.8	11.5	3.90	0.91	3.68	3.18	0.51	99.8	0.0051	4.28	11.0	21.9
Fractionates of the 8% Partial Melt													
10%	58.6	34.1	14.0	5.01	1.14	5.09	4.17	0.61	123.3	0.0050	4.38	11.7	8.18
20%	63.9	22.0	15.7	5.62	1.28	5.70	4.67	0.69	138.5	0.0050	4.38	11.4	4.71
30%	69.0	15.9	17.7	6.33	1.42	6.40	5.26	0.78	151.8	0.0051	4.47	10.9	3.02
Cumulates of the 8% Partial Melt													
10%	50.3	63.2	11.3	4.06	0.93	4.13	3.39	0.5	100.0	0.0050	4.38	12.4	18.6
20%	46.5	69.0	10.1	3.61	0.82	3.67	3.02	0.445	88.9	0.0050	4.38	12.9	22.8
30%	43.4	70.2	8.80	3.16	0.72	3.32	2.67	0.391	78.0	0.0050	4.37	13.7	26.3

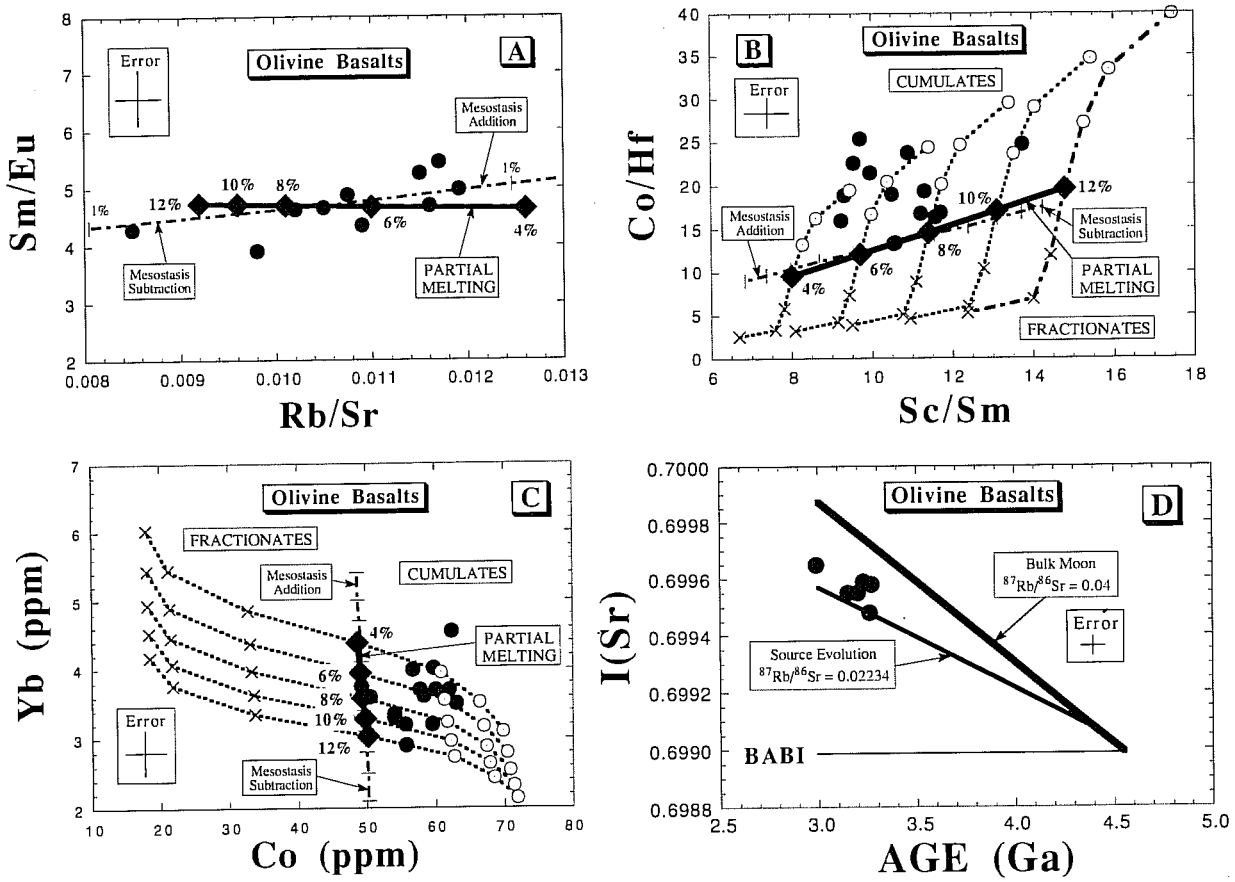

FIG. 7. Source modelling of the Apollo 12 olivine basalts, assuming variable degrees of non-modal batch melting of a source of 48% olivine, 22% pigeonite, and 30% clinopyroxene, melting in the proportions 2.5:2.5:5, followed by closed system crystal fractionation/cumulation. Results are also presented in Table 4. Olivine basalts are represented by the filled circles, and data sources are the same as in Fig. 1. Parental melts produced by variable degrees of partial melting are represented by filled diamonds. The effects of crystal fractionation (crosses) and crystal cumulation (open circles with a dot in the center) are also shown, with each symbol representing 10% crystal fractionation/cumulation up to a maximum of 30%. Results of the modelling are also presented in Table 3. Also shown are the effects of short-range unmixing via mesostasis migration (addition/subtraction). Each path is calculated for 5% mesostasis addition/subtraction, in 1% increments, from the parental composition. Fractionating/accumulating phases are the same as in Table 1 (see text for details). A source evolution path has been calculated using $^{87}Rb/^{86}Sr$ ratio calculated from our source modelling and the $^{87}Sr/^{86}Sr$ ratio of 12015 (data from Bottino *et al.*, 1971; Compston *et al.*, 1971; Murthy *et al.*, 1971; Nyquist *et al.*, 1977, 1979; Papanastassiou and Wasserburg, 1970, 1971). (A) Sm/Eu *vs.* Rb/Sr; (B) Co/Hf *vs.* Sc/Sm; (C) Yb (ppm) *vs.* Co (ppm); and (D) I(Sr) *vs.* Age (Ga).

(1988), no ilmenite is required in our model source. More than one parent and variable degrees of partial melting are required in order to account for the variation in Rb/Sr ratio (0.008–0.012) (Fig. 7a). As the fractionation assemblage will not produce any variation in Rb/Sr and Sm/Eu ratios, the calculated crystal-fractionation/accumulation trends plot directly on top of the calculated melt compositions in Fig. 7a and Table 4. Although the basalt compositions do not fall directly on the partial melting line in Fig. 7a, the observed scatter can be accounted for by analytical precision (primarily in Sm/Eu, as Rb/Sr ratios were analyzed by isotope dilution).

The applicability of this model to the Apollo 12 olivine basalts is seen in Fig. 7b,c. In each case, the olivine basalts are successfully generated by parental magmas generated by 5% to 11% partial melting of the calculated source (similar to Hughes *et al.*, 1988), followed by generally ≤25% crystal accumulation. All basalt compositions plot on the cumulate side of the partial melting path, which is consistent with earlier observations (James and Wright, 1972; Walker *et al.*, 1976; Rhodes *et al.*, 1977).

The possibility that open-system behavior has produced the observed trace-element variations can be addressed by examining existing Apollo 12 olivine basalt Sr and Nd isotope data (Bottino *et al.*, 1971; Compston *et al.*, 1971; Murthy *et al.*, 1971; Nyquist *et al.*, 1977, 1979; Papanastassiou and Wasserburg, 1971). As with the ilmenite basalts, initial isotopic ratios were calculated using isochron and ^{40}Ar-^{39}Ar ages (*e.g.*, Alexander *et al.*, 1972; Stettler *et al.*, 1973). The evolution of the olivine basalt source was calculated using the Rb/Sr ratio obtained from the trace-element modelling and the $^{87}Sr/^{86}Sr$ ratio of 12015 (Nyquist *et al.*, 1977). The olivine basalts generally plot within error of this model path (Fig. 7d). This two-stage evolution model may oversimplify source development but demonstrates that the olivine basalts have similar initial Sr isotopic ratios, which is consistent with a closed-system petrogenesis. Calculation of a Nd isotope evolution path for our estimated source could not be undertaken as no Nd isotope data are available for the vitrophyric (parental) olivine basalts. However, the whole-rock data reported by Nyquist *et al.* (1979) for two olivine basalts (12014 and 12076) indicate similar present day

(0.512312 ± 17 and 0.512301 ± 21, respectively) and initial $^{143}Nd/^{144}Nd$ ratios (0.50787 ± 15 and 0.50783, respectively), suggesting evolution through closed-system processes.

Can Short-Range Unmixing Generate Observed Apollo 12 Basalt Compositions?

The validity of the above modelling would be severely diminished if the observed compositional ranges of the Apollo 12 mare basalts can be attributed to short-range unmixing (Haskin *et al.*, 1977; Lindstrom and Haskin, 1978, 1981). The ratios used in the modelling will also be affected by such short-range unmixing through residual melt (mesostasis) migration. Modelling of such mesostasis migration was undertaken assuming a high-K KREEP composition (Warren and Wasson, 1979) for this residual melt. In Figs. 4, 6, and 7, evolution paths are represented for addition/subtraction of 5% mesostasis from the parental composition for each of the pigeonite, ilmenite, and olivine basalts.

TABLE 4. Trace-element petrogenetic modelling of the Apollo 12 olivine basalts *via* different degrees of partial melting followed by closed-system crystal fractionation/accumulation. Results are in ppm.

	Sc	Co	Ce	Sm	Eu	Yb	Hf	Rb	Sr	Rb/Sr	Sm/Eu	Sc/Sm	Co/Hf
OLIVINE BASALTS													
Source Composition													
(7%)	44.0	146.0	1.34	0.52	0.108	0.65	0.39	0.08	10.3	0.0077	4.83	84.5	374
Parental Melts													
4%	46.3	48.7	26.1	5.77	1.25	4.38	5.07	1.78	141.5	0.0126	4.64	8.00	9.60
6%	46.5	49.1	18.9	4.80	1.03	3.94	4.07	1.23	112.5	0.0110	4.67	9.70	12.1
8%	46.8	49.4	14.8	4.11	0.88	3.58	3.39	0.94	93.3	0.0101	4.70	11.4	14.6
10%	47.1	49.8	12.2	3.59	0.761	3.28	2.91	0.77	79.7	0.0096	4.72	13.1	17.1
12%	47.3	50.2	10.3	3.19	0.674	3.03	2.55	0.64	69.6	0.0092	4.74	14.8	19.7
Fractionates of the 4% Partial Melt													
10%	50.0	32.8	29.0	6.40	1.38	4.85	5.62	1.98	157.1	0.0126	4.63	7.81	5.84
20%	54.5	21.2	32.5	7.19	1.55	5.44	6.30	2.22	176.5	0.0126	4.63	7.51	2.81
30%	53.7	18.0	36.3	8.03	1.73	6.03	7.00	2.48	197.0	0.0126	4.63	6.69	2.57
Cumulates of the 4% Partial Melt													
10%	42.9	60.8	23.5	5.19	1.12	3.95	4.57	1.60	127.4	0.0126	4.63	8.27	13.3
20%	39.7	66.4	20.9	4.62	1.00	3.52	4.08	1.42	113.2	0.0126	4.63	8.60	16.3
30%	38.2	69.8	18.3	4.04	0.87	3.10	3.59	1.25	99.1	0.0126	4.63	9.45	19.5
Fractionates of the 6% Partial Melt													
10%	50.2	33.1	21.0	5.33	1.14	4.37	4.51	1.37	124.9	0.0110	4.67	9.43	7.34
20%	54.8	21.4	23.6	5.98	1.28	4.89	5.06	1.54	140.3	0.0110	4.67	9.15	4.22
30%	53.9	18.1	26.3	6.68	1.43	5.43	5.62	1.72	156.6	0.0110	4.67	8.08	3.23
Cumulates of the 6% Partial Melt													
10%	43.1	61.3	17.0	4.32	0.93	3.55	3.67	1.11	101.3	0.0110	4.67	9.98	16.7
20%	39.9	67.0	15.1	3.84	0.82	3.17	3.27	0.99	90.0	0.0110	4.67	10.4	20.5
30%	38.4	70.4	13.2	3.36	0.72	2.79	2.88	0.86	78.8	0.0110	4.67	11.4	24.4
Fractionates of the 8% Partial Melt													
10%	50.6	33.3	16.4	4.56	0.97	3.97	3.76	1.05	103.6	0.0101	4.70	11.1	8.86
20%	55.1	21.5	18.5	5.12	1.09	4.45	4.21	1.18	116.3	0.0101	4.70	10.8	5.10
30%	54.3	18.2	20.6	5.72	1.22	4.93	4.68	1.31	129.9	0.0101	4.70	9.50	3.90
Cumulates of the 8% Partial Melt													
10%	43.4	61.7	13.3	3.70	0.79	3.23	3.06	0.85	84.0	0.0101	4.70	11.7	20.2
20%	40.1	67.4	11.8	3.29	0.70	2.88	2.73	0.76	74.6	0.0101	4.70	12.2	24.7
30%	38.6	70.8	10.4	2.88	0.61	2.54	2.40	0.66	65.3	0.0101	4.70	13.4	29.5
Fractionates of the 10% Partial Melt													
10%	50.9	33.6	13.5	3.98	0.84	3.63	3.22	0.85	88.5	0.0096	4.72	12.8	10.4
20%	55.5	21.7	15.2	4.48	0.95	4.07	3.62	0.95	99.4	0.0096	4.72	12.4	5.99
30%	54.6	18.4	17.0	4.99	1.06	4.52	4.02	1.07	111.0	0.0096	4.72	10.9	4.58
Cumulates of the 10% Partial Melt													
10%	43.7	62.2	11.0	3.23	0.68	2.96	2.62	0.69	71.7	0.0096	4.72	13.5	23.7
20%	40.4	67.9	9.80	2.87	0.61	2.64	2.34	0.61	63.8	0.0096	4.72	14.1	29.0
30%	38.9	71.4	8.50	2.52	0.53	2.32	2.06	0.54	55.8	0.0096	4.72	15.5	34.7
Fractionates of the 12% Partial Melt													
10%	51.1	33.8	11.4	3.54	0.75	3.35	2.83	0.71	77.3	0.0092	4.73	14.4	12.0
20%	55.7	21.8	12.8	3.98	0.84	3.76	3.17	0.80	86.8	0.0092	4.73	14.0	6.89
30%	54.9	18.5	14.3	4.44	0.94	4.17	6.52	0.90	96.9	0.0092	4.73	12.4	5.27
Cumulates of the 12% Partial Melt													
10%	43.9	62.7	9.30	2.87	0.61	2.73	2.30	0.58	62.6	0.0092	4.73	15.3	27.2
20%	40.6	68.5	8.20	2.55	0.54	2.43	2.05	0.51	55.7	0.0092	4.73	15.9	33.4
30%	39.0	71.9	7.20	2.24	0.47	2.14	1.80	0.45	48.7	0.0092	4.73	17.5	39.9

While it is evident that the range in Rb/Sr and Sm/Eu ratios for the pigeonite (Fig. 4b), ilmenite (Fig. 6a), and the olivine basalts (Fig. 7a) can be generated by such mesostasis migration, other ratios (Co/Hf, Sc/Sm) as well as elemental abundances cannot be generated in such a way (Fig. 4a,c,d; Fig. 6b,c; Fig. 7b,c). This evidence clearly indicates that the compositional ranges observed in each of the three Apollo 12 mare basalt suites are not due to short-range unmixing.

SUMMARY

The chemistry of the pigeonite basalts cannot be reconciled with a petrogenesis involving variable degrees of partial melting and/or closed-system crystal fractionation/accumulation. Explanation of major- and trace-element data require assimilation of anorthositic lunar crust by a parental magma represented by vitrophyre 12011. The composition of the assimilant is non-unique, in keeping with the heterogeneous nature of the lunar crust on the western near-side. However, the contaminant must have been Al-, Sr-, and Eu-rich (anorthositic), with low Sm/Eu and Rb/Sr ratios, and REE-poor. Using end-member literature values for the anorthositic assimilant (>29 wt% Al_2O_3), an "AFC band" has been calculated. In order to account for the data, an "r" value of 0.3 is required, and the pigeonite basalts are generated after 10% fractional crystallization (3% assimilation). Only 12031 requires variable amounts of AFC (depending upon the chemical parameters used), but this analysis is not representative of the whole-rock composition (Neal *et al.*, 1994).

It is evident from major-element compositions that crystal fractionation/accumulation has played an important role in the petrogenesis of the olivine and ilmenite basalts. However, trace-element ratios and abundances indicate that more than one parental melt is required. The major- and trace-element data can be reconciled by variable degrees of partial melting of a source containing early- and late-stage crystallization products of the LMO, supporting an overturning of the mantle cumulate pile, but the scale of this overturn is equivocal. The ilmenite source is composed of 45.5% olivine + 42.5% pigeonite + 11.5% clinopyroxene + 0.5% plagioclase melting in the proportions of 1.5:4.5:3.5:0.5. In order to generate the compositions of the ilmenite basalts, variable degrees of partial melting of this source (between 2% and 8%) are required followed by crystal fractionation and accumulation. The olivine source is composed of 48% olivine, 22% pigeonite, and 30% clinopyroxene, melting in the proportions 2.5:2.5:5. In order to generate the compositions of the olivine basalts, between 5% and 11% partial melting of this source is required, followed by crystal accumulation. The evolved liquid counterparts of these cumulates have not been sampled. In melting the sources for both the ilmenite and olivine basalts, none of the minerals are exhausted after the degrees of partial melting postulated here.

Acknowledgements–This paper has been greatly improved by thorough reviews by Chip Shearer, John Longhi, and Paul Warren. The study has been supported through NASA grant NAG 9-415 to L.A.T., a Notre Dame *Jesse H. Jones* Research Fellowship to C.R.N. and M.D.H., and NASA grant NAG 9-63 to R.A.S.

Editorial handling: P. Warren

REFERENCES

ALEXANDER E. C., JR., DAVIS P. K. AND REYNOLDS J. H. (1972) Rare-gas analyses on neutron irradiated Apollo 12 samples. *Proc. Lunar Planet. Sci. Conf.* **3rd,** 1787–1795.

BALDRIDGE W. S., BEATY D. W., HILL S. M. R. AND ALBEE A. L. (1979) The petrology of the Apollo 12 pigeonite basalt suite. *Proc. Lunar Planet. Sci. Conf.* **10th,** 141–179.

BEATY D. W., HILL S M. R., ALBEE A. L. AND BALDRIDGE W. S. (1979) Apollo 12 feldspathic basalts 12031, 12038, and 12072: Petrology, comparison, and interpretation. *Proc. Lunar Planet. Sci. Conf.* **10th,** 115–139.

BOTTINO M. L., FULLAGAR P. D., SCHNETZLER C. C. AND PHILPOTTS J. A. (1971) Sr isotopic measurements in Apollo 12 samples. *Proc. Lunar Planet. Sci. Conf.* **2nd,** 1487–1491.

BRUNFELT A. O., HEIER K. S. AND STEINNES E. (1971) Determination of 40 elements in Apollo 12 materials by neutron activation analysis. *Proc. Lunar Planet. Sci. Conf.* **2nd,** 1281–1290.

COMPSTON W., BERRY H., VERNON M. J., CHAPPELL B. W. AND KAYE M. J. (1971) Rubidium-strontium chronology and chemistry of lunar material from the Ocean of Storms. *Proc. Lunar Planet. Sci. Conf.* **2nd,** 1471–1485.

CUTTITTA F., ROSE H. J., JR., ANNELL C. S., CARRON M. K., CHRISTIAN R. P., DWORNIK E. J., GREENLAND L. P., HELZ A. P. AND LIGON D.T., JR. (1971) Elemental composition of some Apollo 12 lunar rocks and soils. *Proc. Lunar Planet. Sci. Conf.* **2nd,** 1217–1229.

DEPAOLO D. J. (1981) Trace-element and isotopic effects of combined wallrock assimilation and fractional crystallization. *Earth Planet. Sci. Lett.* **53,** 189–202.

DUNGAN M. A. AND BROWN R. W (1977) The petrology of the Apollo 12 ilmenite basalt suite. *Proc. Lunar Planet. Sci. Conf.* **8th,** 1339–1381.

ENGEL A. E. J., ENGEL C. G., SUTTON A. L. AND MYERS A. T. (1971) Composition of five Apollo 11 and Apollo 12 rocks and one Apollo 11 soil and some petrogenetic considerations. *Proc. Lunar Planet. Sci. Conf.* **2nd,** 439–448.

FINILLA A. B., HESS P. C. AND RUTHERFORD M. J. (1993) Assimilation in lunar basalts and volcanic glasses: Implications for a heterogeneous mantle source region (abstract). *Lunar Planet. Sci.* **24,** 475–476.

FINILLA A. B., HESS P. C. AND RUTHERFORD M. J. (1994 Assimilation by lunar basalts: Melting of crustal material and dissolution of anorthite. *J. Geophys. Res.*, submitted.

GOODRICH C. A., TAYLOR G. J., KEIL K., KALLEMEYN G. W. AND WARREN P. H. (1986) Alkali norite, troctolites, and VHK mare basalts from breccia 14304. *Proc. Lunar Planet. Sci. Conf.* **16th,** *J. Geophys. Res.* **91,** D305–D318.

GREEN D. H., RINGWOOD A. E., WARE N. G., HIBBERSON W. O., MAJOR A. and KISS E. (1971) Experimental petrology and petrogenesis of Apollo 12 basalts. *Proc. Lunar Planet. Sci. Conf.* **2nd,** 601–615.

HASKIN L. A., HELMKE P. A., ALLEN R. O., ANDERSON M. R., KOROTEV R. L. AND ZWEIFEL K. A. (1971) Rare-earth elements in Apollo 12 lunar materials. *Proc. Lunar Planet. Sci. Conf.* **2nd,** 1307–1317.

HASKIN L. A., JACOBS J. W., BRANNON J. C. AND HASKIN M. A. (1977) Compositional dispersions in lunar and terrestrial basalts. *Proc. Lunar Planet. Sci. Conf.* **8th,** 1731–1750.

HESS P. C. (1991) Pristine mare glasses: Primary magmas? Workshop on: *Mare Volcanism and Basalt Petrogenesis* , pp. 17–18. LPI Technical Report 91-03. Lunar and Planetary Institute, Houston, Texas.

HESS P. C. (1993) The ilmenite liquidus and depths of segregation for high-Ti picrite glasses (abstract). *Lunar Planet. Sci.* **24,** 649–650.

HUBBARD N. J. AND GAST P.W. (1971) Chemical composition and origin of nonmare lunar basalts. *Proc. Lunar Planet. Sci. Conf.* **2nd,** 999–1020.

HUGHES S. S., DELANO J. W. AND SCHMITT R. A. (1988) Apollo 15 yellow-brown volcanic glass: Chemistry and petrogenetic relations to green volcanic glass and olivine-normative mare basalts. *Geochim. Cosmochim. Acta* **52,** 2379–2391.

JAMES O. B. AND WRIGHT T. L. (1972) Apollo 11 and 12 mare basalts and gabbros: Classification, compositional variations, and possible petrogenetic relations. *Bull. Geol. Soc. Am.* **83,** 2357–2382.

KESSON S. E. (1975) Mare basalts: Melting experiments and petrogenetic interpretations. *Proc. Lunar Planet. Sci. Conf.* **6th,** 921–944.

KHARKAR D. P. AND TUREKIAN K. K. (1971) Analyses of Apollo 11 and Apollo 12 rocks and soils by neutron activation. *Proc. Lunar Planet. Sci. Conf.* **2nd,** 1301–1305.

KUSHIRO I. AND HARAMURA H. (1971) Major element variation and possible source materials of Apollo 12 crystalline rocks. *Science* **171,** 1235–1237.

LINDSTROM M. M. AND HASKIN L. A. (1978) Causes of compositional variation within mare basalt suites. *Proc. Lunar Planet. Sci. Conf.* **9th,** 465–486.

LINDSTROM M. M. AND HASKIN L. A. (1981) Compositional inhomogeneities in a single Icelandic tholeiite flow. *Geochim. Cosmochim. Acta* **45,** 15–31.

LINDSTROM M. M., KNAPP S. A., SHERVAIS J. W. AND TAYLOR L. A. (1984) Magnesian anorthosites - a new rock type from Apollo 14. *Proc. Lunar Planet. Sci. Conf.* **15th,** *J. Geophys. Res.* **90,** C41–C49.

LONGHI J. (1987) On the connection between mare basalts and picritic volcanic glasses. *Proc. Lunar Planet. Sci. Conf.* **17th,** *J. Geophys. Res.* **92,** E349–E360.

LONGHI J. (1991) Comparative liquidus equilibria of hypersthene-normative basalts at low pressure. *Amer. Mineral.* **76,** 785–800.

LONGHI J. (1992) Origin of picritic green glass magmas by polybaric fractional fusion. *Proc. Lunar Planet. Sci. Conf.* **22nd,** 343–353.

LONGHI J., WALKER D., GROVE T. L., STOLPER E. M. AND HAYS J. F. (1974) The petrology of the Apollo 17 mare basalts. *Proc. Lunar Planet. Sci. Conf.* **5th,** 447–469.

LSPET (Lunar Sample Preliminary Examination Team) (1970) Preliminary examination of the lunar samples from Apollo 12. *Science* **167,** 1325–1339.

LUGMAIR G. W. (1974) Sm-Nd ages: A new dating method (abstract). *Meteoritics* **9,** 369.

LUGMAIR G. W., MARTI K., KURTZ J. P. AND SCHEININ N. B. (1976) History and genesis of lunar troctolite 76535 or: How old is old? *Proc. Lunar Planet. Sci. Conf.* **7th,** 2009–2033.

MA M.-S., MURALI A. V. AND SCHMITT R. A. (1976) Chemical constraints for mare basalt genesis. *Proc. Lunar Planet. Sci. Conf.* **7th,** 1673–1695.

MAXWELL J. A. AND WIIK H. B. (1971) Chemical composition of Apollo 12 lunar samples 12004, 12033, 12051, 12052, and 12065. *Earth Planet. Sci. Lett.* **10,** 285–288.

MORRISSON G. H., GERARD J. T., POTTER N. M., GANGADHARAM E. V., ROTHENBERG A. M. AND BURDO R. A. (1971) Elemental abundances of lunar soil and rocks from Apollo 12. *Proc. Lunar Planet. Sci. Conf.* **2nd,** 1169–1185.

MURTHY V .R., EVENSEN N. M., JAHN B. M. AND COSCIO M. R., JR. (1971) Rb-Sr ages and elemental abundances of K, Rb, Sr, and Ba in samples from the Ocean of Storms. *Geochim. Cosmochim. Acta* **35,** 1139–1153.

NEAL C. R. AND TAYLOR L. A. (1992) Petrogenesis of mare basalts: A record of lunar volcanism. *Geochim. Cosmochim. Acta* **56,** 2177–2211.

NEAL C. R., TAYLOR L. A. AND LINDSTROM M. M. (1988) Apollo 14 mare basalt petrogenesis: Assimilation of KREEP-like components by a fractionating magma. *Proc. Lunar Planet. Sci. Conf.* **18th,** 139–153.

NEAL C. R., TAYLOR L. A. AND LINDSTROM M. M. (1991) Problems inherent in the study of lunar highland samples: The "typical case" at Apollo 14 (abstract). *Lunar Planet. Sci.* **22,** 969–970.

NEAL C. R., HACKER M. D., TAYLOR L. A., SCHMITT R. A. AND LIU Y.-G. (1994) Basalt generation at the Apollo 12 site, part 1: New data, classification, and re-evaluation. *Meteoritics* **29,** 349–361.

NYQUIST L .E. (1977) Lunar Rb-Sr chronology. *Phys. Chem. Earth* **10,** 103–142.

NYQUIST L. E. AND SHIH C.-Y. (1992) On the chronology and isotopic record of lunar basaltic volcanism. *Geochim. Cosmochim. Acta* **56,** 2213–2234.

NYQUIST L. E., BANSAL B. M., WOODEN J. L. AND WIESMANN H. (1977) Sr-isotopic constraints on the petrogenesis of Apollo 12 mare basalts. *Proc. Lunar Planet. Sci. Conf.* **8th,** 1383–1415.

NYQUIST L E., SHIH C.-Y., WOODEN J. L., BANSAL B. M. AND WIESMANN H. (1979) The Sr and Nd isotopic record of Apollo 12 basalts: Implications for lunar geochemical evolution. *Proc. Lunar Planet. Sci. Conf.* **10th,** 77–114.

NYQUIST L. E., WOODEN J. L., SHIH C.-Y., WIESMANN H. AND BANSAL B. M. (1981) Isotopic and REE studies of lunar basalt 12038: Implications for petrogenesis of aluminous mare basalts. *Earth Planet. Sci. Lett.* **55,** 335–355.

PAPANASTASSIOU D. A. AND WASSERBURG G. J. (1970) Rb-Sr ages from the Ocean of Storms. *Earth Planet. Sci. Lett.* **8,** 269–278.

PAPANASTASSIOU D. A. AND WASSERBURG G. J. (1971) Lunar chronology and evolution from Rb-Sr studies of Apollo 11 and 12 samples. *Earth Planet. Sci. Lett.* **11,** 37–62.

PAPIKE J. J. AND VANIMAN D. T. (1978) Luna 24 ferrobasalts and the mare basalt suite: Comparative chemistry, mineralogy, and petrology. In *Mare Crisium: The View from Luna 24* (eds. R. B. Merrill and J. J. Papike), pp. 371–401. Pergamon, New York..

PAPIKE J. J., HODGES F. N., BENCE A. E., CAMERON M. AND RHODES J. M. (1976) Mare basalts: Crystal chemistry, mineralogy, and petrology. *Rev. Geophys. Space Phys.* **14,** 475–540.

RHODES J. M., BLANCHARD D. P., DUNGAN M. A., BRANNON J. C. AND RODGERS K. V. (1977) Chemistry of Apollo 12 mare basalts: Magma types and fractionation processes. *Proc. Lunar Planet. Sci. Conf.* **8th,** 1305–1338.

RINGWOOD A. E. AND KESSON S. E. (1976) A dynamic model for mare basalt petrogenesis. *Proc. Lunar Planet. Sci. Conf.* **7th,** 1697–1722.

SCHNETZLER C. C. AND PHILPOTTS J. A. (1971) Alkali, alkaline earth, and rare-earth element concentrations in some Apollo 12 soils, rocks, and separated phases. *Proc. Lunar Planet. Sci. Conf.* **2nd,** 1101–1122.

SCOON J. H. (1971) Chemical analyses of lunar samples 12040 and 12064. *Proc. Lunar Planet. Sci. Conf.* **2nd,** 1259–1260.

SHEARER C .K. AND PAPIKE J. J. (1993) Basaltic magmatism on the Moon: A perspective from volcanic picritic glass beads. *Geochim. Cosmochim. Acta* **57,** 4785–4812.

SHERVAIS J. W., TAYLOR L. A., LAUL J. C. AND SMITH M. R. (1984) Pristine highland clasts in consortium breccia 14305: Petrology and geochemistry. *Proc. Lunar Planet. Sci. Conf.* **15th,** *J. Geophys. Res.* **89,** C25–C40.

SHIH C.-Y. AND SCHONFELD E. (1976) Mare basalt genesis: A cumulate re-melting model. *Proc. Lunar Planet. Sci. Conf.* **7th,** 1757–1792.

SNYDER G. A., TAYLOR L. A. AND NEAL C. R. (1992) A chemical model for generating the sources of mare basalts: Imperfect, geologically realistic fractional crystallization of the lunar magmasphere. *Geochim. Cosmochim. Acta* **56,** 3809–3823.

SPERA F. J. (1991) Lunar magma transport phenomena. *Lunar and Planetary Institute Tech. Rept.* **91-03,** 55–58.

SPERA F. J. (1992) Lunar magma transport phenomena. *Geochim. Cosmochim. Acta* **56,** 2253–2265.

STETTLER A., EBERHARDT P., GEISS J., GRÖGLER N. AND MAURER P. (1973) Ar^{39}-Ar^{40} ages and Ar^{37}-Ar^{38} exposure ages of lunar rocks. *Proc. Lunar Planet. Sci. Conf.* **4th,** 1865–1888.

TAYLOR S. R. (1982) *Planetary Science: A Lunar Perspective.* The Lunar and Planetary Institute, Houston, Texas. 481 pp..

TAYLOR S R., RODOWSKI R., MUIR P., GRAHAM A. AND KAYE M. (1971) Trace element chemistry of lunar samples from the Ocean of Storms. *Proc. Lunar Planet. Sci. Conf.* **2nd,** 1083–1099.

UNRUH D. M., STILLE P., PATCHETT P. J. AND TATSUMOTO M. (1984) Lu-Hf and Sm-Nd evolution in lunar mare basalts. *Proc. Lunar Planet. Sci. Conf.* **14th,** *J. Geophys. Res.* **89,** B459–B477.

VOBECKY M., FRANA J., BAUER J., RANDA Z., BENADA J. AND KUNCIR J. (1971) Radioanalytical determination of elemental compositions of lunar samples. *Proc. Lunar Planet. Sci. Conf.* **2nd,** 1291–1300.

WAKITA H. and SCHMITT R.A. (1971) Bulk elemental composition of Apollo 12 samples: Five igneous and one breccia rock and four soils. *Proc. Lunar Planet. Sci. Conf.* **2nd,** 1231–1236.

WAKITA H., REY P. AND SCHMITT R. A. (1971) Abundances of the 14 rare-earth elements and 12 other trace elements in Apollo 12 samples: Five igneous and one breccia rocks and four soils. *Proc. Lunar Planet. Sci. Conf.* **2nd,** 1319–1329.

WALKER D., LONGHI J., KIRKPATRICK R. J. AND HAYS J .F. (1976) Differentiation of an Apollo 12 picrite magma. P*roc. Lunar Planet. Sci. Conf.* **7th,** 1365–1389.

WÄNKE H., WLOTZKA F., BADDENHAUSEN H., BALACESCU A., SPETTEL B., JAGOUTZ E., KRUSE H., QUIJANO-RICO M. AND RIEDER R. (1971) Apollo 12 samples: Chemical composition and its relation to sample locations and exposure ages, the two component origin of the various soil samples and studies on lunar metallic particles. *Proc. Lunar Planet. Sci. Conf.* **2nd,** 1187–1208.

WARREN P. H. (1985) The magma ocean concept and lunar evolution. *Ann. Rev. Earth Planet. Sci.* **13,** 201–240.

WARREN P .H. (1986) Anorthosite assimilation and the origin of the Mg/Fe-related bimodality of pristine Moon rocks: Support for the magmasphere hypothesis. *Proc. Lunar Planet. Sci. Conf.* **16th,** *Jour. Geophys. Res.* **91,** D331–D343.

WARREN P. H. AND WASSON J. T. (1979) The origin of KREEP. *Rev. Geophys. Space Phys.* **17,** 73–88

WARREN P. H., TAYLOR G. J., KEIL K., KALLEMEYN G. W., ROSENER P. S. AND WASSON J. T. (1983) Sixth foray for pristine nonmare rocks and an assessment of the diversity of lunar anorthosites. *Proc. Lunar Planet. Sci. Conf.* **13th,** *J. Geophys. Res.* **13,** A615–A630.

WARREN P. H., JERDE E. A. AND KALLEMEYN G. W. (1990) Pristine Moon rocks: An alkali anorthosite with coarse augite exsolution from plagioclase, a magnesian harzburgite, and other oddities. *Proc. Lunar Planet. Sci. Conf.* **20th,** 31–59.

WILLIS J. P., AHRENS L. H., DANCHIN R. V., ERLANK A. J., GURNEY J. J., HOFMEYR P. K., MCCARTHY T. S. AND ORREN M. J. (1971) Some inter-element relationships between lunar rocks and fines, and stony meteorites. *Proc. Lunar Planet. Sci. Conf.* **2nd,** 1123–1138